

# Shattered Pellet Injection experiments at ASDEX-Upgrade for design optimisation of the ITER Disruption Mitigation System

S. Jachmich<sup>1</sup>, M. Lehnen<sup>1</sup>, G. Papp<sup>2</sup>, M. Dibon<sup>1,2</sup>, P. Heinrich<sup>2</sup>, U. Kruezi<sup>1</sup>, P. de Marné<sup>2</sup>, M. Bernert<sup>2</sup>, A. Bock<sup>2</sup>, J. Cerovsky<sup>3</sup>, O. Ficker<sup>3</sup>, D. Fiorucci<sup>4</sup>, G. Kocsis<sup>5</sup>, B. Kurzan<sup>2</sup>, A. Lukin<sup>6</sup>, T. Peherstorfer<sup>7</sup>, U. Sheikh<sup>8</sup>, I Vinyar<sup>6</sup>, T. Eich<sup>2</sup>, J. Hobirk<sup>2</sup>  
and the ASDEX Upgrade Team\*

<sup>1</sup> ITER Organization, Route de Vinon, CS 90 046, 13067 Saint Paul Lez Durance, France

<sup>2</sup> Max-Planck-Institut für Plasma Physik, D-85748, Garching, Germany

<sup>3</sup> Institute of Plasma Physics of the CAS, Prague, Czech Republic

<sup>4</sup> ENEA research center Frascati, Via Enrico Fermi 45, 00044 Rome, Italy

<sup>5</sup> Centre for Energy Research, Budapest, Hungary

<sup>6</sup> PELIN, LLC., 27A, Gzhatskaya, Saint-Petersburg, 195220, Russian Federation

<sup>7</sup> Vienna University of Technology, Vienna, Austria

<sup>8</sup> Ecole Polytechnique Fédérale de Lausanne, Swiss Plasma Center (SPC), CH-1015 Lausanne, Switzerland

\* see author list of U. Stroth et al. Nucl Fus 62, 042006, 2022

## 1. Introduction

ITER is planning to install a disruption mitigation system (DMS), which is essential to protect the machine against detrimental effects resulting from disruptions [1]. To fulfil this task, the DMS will consist of several shattered pellet injectors (SPI) to deliver neon (Ne) and a large quantity of protium (H) in the form of fragments to the plasma. The fragment size and velocity distribution and spatial spread of the plume are governed by the chosen shattering unit geometry and the velocity of the impacting pellet. The specifications for the DMS shattering unit are determined in a concerted effort through modelling to predict the optimum fragment injections for ITER, experiments on existing tokamaks, and design testing in dedicated laboratories. In order to study the effects of different fragment plume characteristics on the material assimilation efficiency, a triple barrel SPI equipped with three different shattering units, together with new bolometric systems and fast cameras observing the injection location were installed on ASDEX-Upgrade (AUG) as part of the ITER DMS Task Force activities [2]. This paper summarises different type of injections with the SPI into a range of target plasmas, which were carried out during the 2022 AUG campaign.

## 2. SPI system capabilities

The SPI is installed on the low field side above the midplane to ensure that the shatter heads are pointing towards the plasma core (see Figure 1). The injector has three barrels with separate flight tubes, which terminate in individual shatter heads. Each injector line can be equipped with barrels having a diameter,  $D$  of 1, 2, 4 or 8 mm. The experiments reported here were carried out with 4 and 8 mm pellets. The length,  $L$  of pellets can be varied by using barrel heaters over the range  $L/D \sim 0.5$ -1.6 corresponding to a content of  $0.5$ - $3.0 \times 10^{22}$  deuterium (D) atoms. By using a hollow punch system together with a propellant valve [3], the velocity of D-pellets can be controlled from  $\sim 120$  to  $\sim 770$  m/s. Pellets with substantial Ne-content are accordingly slower due

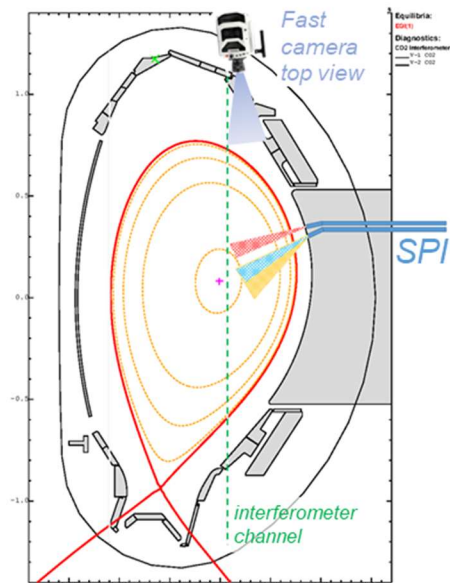


**Figure 1:** Cross-section of plasma equilibrium and SPI injection geometries. In addition, the position of the two-colour laser interferometer channel and the fast camera observation of the injected fragments are indicated.

to their higher mass. Expansion volumes amounting to a total of  $0.33 \text{ m}^3$  are connected to the flight tubes to capture the propellant such that any adverse effect of the early arrival of propellant gas on the target plasma is avoided. Two flight tubes were equipped with shatter heads having a rectangular cross-section to guarantee a well-defined impact angle. The two shattering angles  $\alpha$  of  $12.5^\circ$  and  $25.0^\circ$  were chosen such that by matching the impact velocity  $v_\perp$ , defined as  $v_\perp = v_{\text{pellet}} \times \sin(\alpha)$ , a similar fragment size distribution can be injected with different velocities. In the data presented below,  $v_\perp$  is used as a proxy for the average fragment size. To study the effect of a fragment plume with a wider spread perpendicular to the injection direction, a shorter head with a circular cross-section and a shattering angle of  $25.0^\circ$  was installed on the third flight tube. Prior to the installation in the torus, the fragment plumes for the different shatter heads were characterised in the laboratory [4]. More details on the SPI system can be found in [5].

### 3. Experiments for assessing SPI material assimilation

One of the disruption mitigation tasks of the ITER DMS is to raise the density sufficiently by the time of the thermal quench (TQ) to avoid the formation of runaway electrons during the subsequent current quench (CQ). The main aim of the AUG-SPI experiments was to determine the amount of assimilated material injected with the SPI into various target plasmas. All injections reported here were performed into the steady-state phase of two target plasmas, ohmic ( $q_{95} \sim 3.6$ ) and standard H-mode ( $q_{95} \sim 3.7$ ) with respectively thermal energies.  $W_{\text{MHD}}$  of  $\sim 100$  and  $600 \text{ kJ}$ . The particle content in these plasmas was similar and about  $5.5\text{-}6.3 \times 10^{20}$ . These plasmas had similar core density profiles and the central plasma core temperature in the H-mode plasmas was  $\sim 5.5 \text{ keV}$  compared to only  $1 \text{ keV}$  in ohmic. Before the injection, these plasmas can be considered free of any instability, in particular any  $n=1$  mode. Figure 2 shows the typical sequence of events for a pure deuterium injection into a standard H-mode plasma. The SPI is triggered at  $2.353 \text{ s}$  and after about  $10 \text{ ms}$  of flight time, the fragments appear in the plasma as inferred from the signal rise of an AXUV-diode intersecting with the fragment plume at  $R \sim 2.15 \text{ m}$ . Coinciding with an initial short phase of enhanced radiation, the plasma energy drops by about  $150 \text{ kJ}$ . Despite the continuous NBI-heating,  $W_{\text{MHD}}$  and plasma current,  $I_p$  decrease further until the formation of an  $n=1$  mode which starts to lock at  $t \sim 2.382 \text{ s}$ . The start of the TQ is indicated by the rise of  $I_p$  prior the CQ. In turn, this coincides approximately with the amplitude of the  $n=1$  mode at the TQ onset as predicted by the scaling in [6]. In the study of this paper, the end of the pre-TQ phase is defined as the time when  $I_p$  is minimum before the start of the CQ. As is typical for disruptions with low radiation, the initial phase of the  $I_p$  decay until the plasma becomes vertically unstable is long due to the low plasma resistivity.

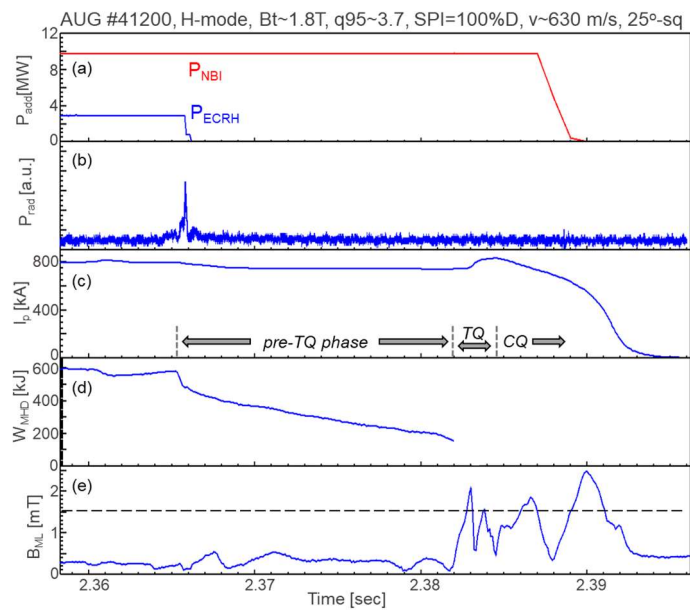


**Figure 2:** Time traces during an SPI into a standard H-mode (a) neutral beam and ECRH power, (b) radiation measured by an AXUV-diode with a LOS intersecting the fragment plume at  $R \sim 2.15 \text{ m}$ , (c) plasma current with different phases of the disruption, (d) plasma energy and (e) amplitude of locked  $n=1$  mode, the dashed line indicating the amplitude at which the TQ is expected to be triggered.

Figure 2 shows the typical sequence of events for a pure deuterium injection into a standard H-mode plasma. The SPI is triggered at  $2.353 \text{ s}$  and after about  $10 \text{ ms}$  of flight time, the fragments appear in the plasma as inferred from the signal rise of an AXUV-diode intersecting with the fragment plume at  $R \sim 2.15 \text{ m}$ . Coinciding with an initial short phase of enhanced radiation, the plasma energy drops by about  $150 \text{ kJ}$ . Despite the continuous NBI-heating,  $W_{\text{MHD}}$  and plasma current,  $I_p$  decrease further until the formation of an  $n=1$  mode which starts to lock at  $t \sim 2.382 \text{ s}$ . The start of the TQ is indicated by the rise of  $I_p$  prior the CQ. In turn, this coincides approximately with the amplitude of the  $n=1$  mode at the TQ onset as predicted by the scaling in [6]. In the study of this paper, the end of the pre-TQ phase is defined as the time when  $I_p$  is minimum before the start of the CQ. As is typical for disruptions with low radiation, the initial phase of the  $I_p$  decay until the plasma becomes vertically unstable is long due to the low plasma resistivity.

#### 4. Assimilation of deuterium SPI

Injections with small (4 mm) D-pellets did not lead to a disruption and the amount of assimilated material did not exceed  $\sim 60\%$  of the original pellet content as indicated by blue symbols in Figure 3, which shows the rise in total electron content as function of impact velocity. The electron content is inferred from the peak density measured by the central channel of the two-colour laser interferometer (c.f. LOS in Figure 1, toroidally  $112^\circ$  away from the SPI). Possible asymmetries in the density could introduce an uncertainty in the measurement.

A trend with impact velocity can be observed for the injections with short 8 mm pellets ( $L \sim 6$  mm). The assimilation increases with decreasing  $v_{\perp}$ , i.e. increasing averaged fragment size (diamond and square symbols). There might be an additional benefit for injections with a larger fragment plume (circles vs. squares). The role of the injection velocity could not be disentangled due to the limited data in this scan.

By using full size 8 mm pellets (content  $\sim 3.0 \times 10^{22}$  D-atoms), the density limit can be reached, causing the plasma to disrupt. The data of this scan are summarised in Figure 4 showing the pre-TQ duration and assimilation fraction based on the maximum density during the pre-TQ measured by the central interferometer channel. The assimilation improves for plasmas at high thermal energy and core temperature (c.f. green, cyan and blue diamonds). However, the pre-TQ phase remains short, not exceeding 4 ms. Long pre-TQ phases are advantageous, since the constraint for synchronous arrival of multiple pellet injections can be relaxed and enable staggered injection schemes aiming at further raising the density prior the TQ. Such conditions could only be achieved for high pellet velocities (red squares) and are generally linked to low assimilation of 25-45%. The assimilation improves for SPI with large fragments and the best assimilation is reached for the lowest impact velocity. The comparison of the data set for the  $12.5^\circ$  and  $25^\circ$  shatter heads reveals a clear benefit of higher injection velocities. The circular and square shatter heads allow an assessment of whether or not a more collimated fragment plume would result in more pellet material being absorbed by the plasma. The results from the standard H-mode SPI pulses indicate that a wide spread plume helps the assimilation.

#### 5. SPI injections of Ne and D mixtures

The assimilation of Ne is difficult to assess due to the very short pre-TQ phases of typically 1-2 ms or less in standard H-mode SPI, once Ne in amounts of  $1.3 \times 10^{19}$  atoms, corresponding to 0.085%

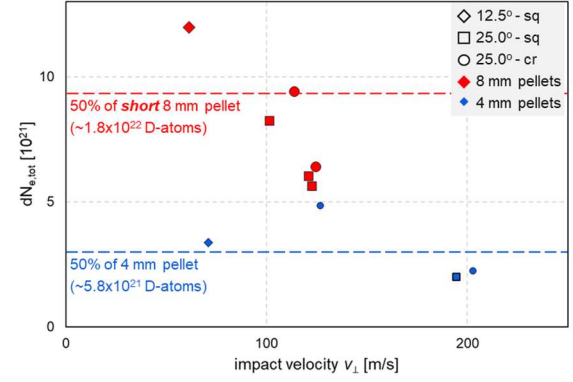


**Figure 3:** Density rise following single SPI injections into standard H-modes as function of impact velocity. The blue data points correspond to 4 mm pellets with standard  $L/D \sim 1.9$  and the red to 8 mm pellets with  $L/D \sim 0.75$ . The different shapes of the symbols correspond to the different shatter heads.

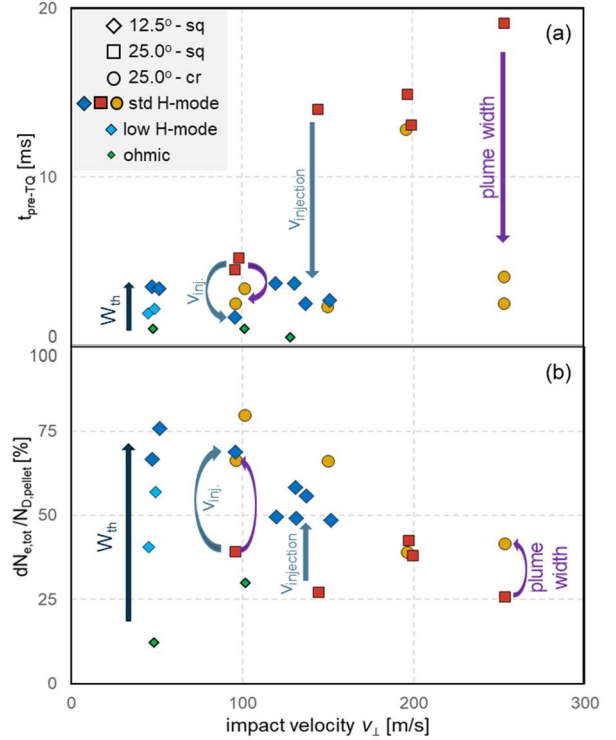


**Figure 4:** (a) Duration of pre-TQ phase for SPI using D-pellets into standard H-modes. Additional data for ohmic (green diamonds) and low thermal energy H-modes ( $\sim 300$  kJ, cyan diamonds) have been acquired. (b) Fraction of pellet content assimilated by the plasma.

of the total atoms in a pellet, is added to D pellets. However, the initial phase of the CQ, while the plasma is still vertically stable, can be used as indicator for the Ne assimilation efficiency. This phase is governed by the plasma resistivity resulting from the balance between ohmic heating and radiation. Here, the time for  $I_p$  to decay to 80% of its value at the start of the CQ, labelled as  $t_{cq,100-80}$ , is used. The analysis is summarised in Figure 5, where  $t_{cq,100-80}$  is shown as function of impact velocity. The Ne quantity has been increased up to  $1.5 \times 10^{21}$  atoms, which is the equivalent of a 10% Ne fraction in the pellet. The shattering geometry and injection velocity have no influence on the initial CQ for large Ne quantities,  $> 1.8 \times 10^{20}$  atoms, indicating an upper limit of the quantity of Ne that can be assimilated. Bolometer analysis has revealed that the radiated fraction, the ratio of radiated energy to the total plasma energy content, saturates once such Ne quantities are injected [7]. For small Ne quantities, a clear effect resulting from fragment sizes and injection velocities can be observed (red and yellow data): large fragments result in the shortest  $t_{cq,100-80}$ . For  $v_{\perp} \sim 100$  m/s, slower injection velocities give poorer assimilation. These findings are consistent with the observations for pure D injections. A wider fragment plume is also found beneficial for Ne injection. The same trend has been observed in the radiation analysis. In the case of SPI with  $2.6 \times 10^{19}$  Ne atoms, the radiated fraction decreases from  $\sim 80\%$  to  $\sim 60\%$  for increasing impact velocities over the explored range [7].

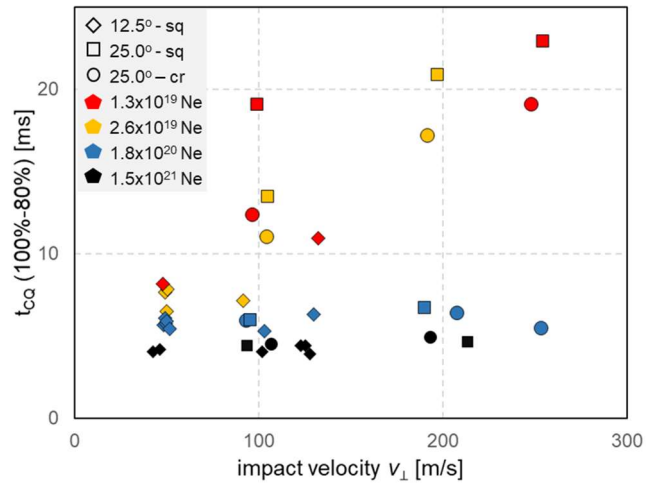


**Figure 5:** Dependence on pellet impact velocity of the time for  $I_p$  to drop by 20% of its value at the start of the CQ for various Ne quantities in D-pellets and shatter head parameters.

## 6. Summary and conclusions

The SPI system on ASDEX Upgrade was used to study the effect of different injection parameters such as fragment sizes, velocities and pellet content on the disruption mitigation efficiency. The highest assimilation has been achieved with injections of large fragments at high velocities. This has been confirmed for D and Ne/D mixed pellets. There might be an additional benefit from a larger fragment plume spread, though this has been investigated for only one shattering angle. The short pre-TQ durations for disruptions with good assimilation following deuterium SPI will pose a constraint on the allowable pellet arrival jitter in the case of multiple injections as foreseen for the ITER DMS. In order to transfer these results to ITER, several modelling validation activities using 1D codes such as INDEX and DREAM, and 3D MHD codes like JOREK are ongoing.

### Acknowledgement and disclaimer

The ASDEX-Upgrade SPI project has been implemented as part of the ITER DMS Task Force programme. The SPI system and related diagnostics have received funding from the ITER Organization under contracts IO/20/CT/43-2084, IO/20/CT/43-2115, IO/20/CT/43-2116. This work has been carried out as a collaboration between the ITER Organization, IPP Garching and the EUROfusion Consortium and its partners, partially funded by the European Union via the Euratom Research and Training Programme (Grant Agreement No 101052200-EUROfusion). Views and opinions expressed are however those of the author(s) only and do not necessarily reflect those of the ITER Organization, European Union or the European Commission. Neither the European Union nor the European Commission can be held responsible for them.

### References

- [1] T. Luce *et al.*, “Progress on the ITER DMS design and integration”. Preprint: 2020 IAEA Fusion Energy Conference, Nice, TECH/I-4Ra.
- [2] M. Lehnen *et al.*, “R&D for reliable disruption mitigation in ITER”. Preprint: 2018 IAEA Fusion Energy Conference, Gandhinagar (India), EX/P7-12.
- [3] I.V. Vinyar *et al.*, Instruments and experimental techniques 57, #4, p 508 (2014).
- [4] T. Peherstorfer, “Fragmentation analysis of cryogenic pellets for disruption mitigation”, MSc Thesis, 2022.
- [5] M. Dibon *et al.*, Rev. Sci. Instrum. 94, 043504 (2023); doi: 10.1063/5.0141799.
- [6] P. de Vries *et al.*, Nucl. Fus. 56, 026007 (2016).
- [7] P. Heinrich *et al.*, this conference, Poster Tu\_MCF54.